Available online at www.sciencedirect.com
SCIENCE DIRECT®
Journal of Power Sources 141 (2005) 122–128
JOURNAL OF POWER SOURCES
www.elsevier.com/locate/jpowsour

Accelerated synthesis and electrochemical performance of $Li_{1+x}(Ni_{0.5}Mn_{0.5})O_{2+\delta}$ cathode materials

O.A. Shlyakhtin[a,b], Sun-Hee Choi[b], Young Soo Yoon[c,*], Young-Jei Oh[b]

[a] *Institute of Chemical Physics, Russian Academy of Sciences, 117334 Moscow, Russia*
[b] *Materials Science and Technology Division, Korea Institute of Science and Technology, Seoul 139-791, Republic of Korea*
[c] *Department of Advanced Technology Fusion (Center for Emerging Wireless Power Transmission Technology), Konkuk University, 1 Hwayang-dong, Gwangjin-gu, Seoul 143-701, Republic of Korea*

Received 30 March 2004; received in revised form 13 August 2004; accepted 13 August 2004
Available online 27 October 2004

Abstract

Synthesis of $Li_{1+x}Ni_{0.5}Mn_{0.5}O_{2+\delta}$ ($x = 0, 0.3$) cathode materials for secondary lithium batteries was performed by freeze-drying method using various chemical precursors. Electrochemical performance of materials demonstrates considerable dependence on their chemical prehistory and Li stoichiometry. Increase in duration of the final annealing at 900 °C since 1–12 h results in decreasing capacity values for all x and chemical prehistories. Observed capacity fall is explained by smaller grain size and, therefore, shorter Li diffusion pathways in the samples obtained using short time annealing.

Keywords: Secondary Li batteries; Cathode materials; Li–Ni–Mn oxides; Freeze-drying; Particle size effect

1. Introduction

Complex Li–Ni–Mn oxides are considered now as promising and inexpensive alternative to $LiCoO_2$ in secondary Li batteries. A solid solution of hexagonal $LiNiO_2$ and $LiMnO_2$, $LiNi_{0.5}Mn_{0.5}O_2$, demonstrates good electrochemical performance and better thermal stability than $LiCoO_2$ [1–7]. A study of $Li[Ni_xLi_{(1/3-2x/3)}Mn_{(2/3-x/3)}]O_2$ compounds, considered as solid solutions of $LiNiO_2$ and Li_2MnO_3, allowed to obtain cathode materials with stable discharge capacity over 200 mAh g^{-1} [8–14]. Similar properties (reversible capacity ~180–190 mAh g^{-1}) was observed for $Li_{1+x}Ni_{0.5}Mn_{0.5}O_{2+\delta}$ ($0 \le x < 0.5$) [15], also having layered hexagonal structure and identified later as $Li[Li_{x/(2+x)}Ni_{1/(2+x)}Mn_{1/(2+x)}]O_{2-\delta}$.

Along with differences, the most of solid solutions in Li–Ni–Mn–O system demonstrate several general features. First of all, it is relatively easy substitution of Li for Ni and Ni for Li in both A and B positions of hexagonal ABO_2 structure due to the small difference of ionic radii of Li^+ and Ni^{2+} [9,16]. Besides, the presence of three different cations in these compounds makes rather complicated the crystallographic ordering processes, necessary for faster transport of Li ions in ABO_2 compounds; clusters with different local environment have been detected in Li–Ni–Mn oxides even after 1 day annealing at 900 °C [17]. One of the main obstacles to crystallographic ordering is easy and selective formation of Li_2MnO_3 during thermal decomposition of various chemical precursors [18], which makes rather complicated further chemical homogenization of the system during following processing of materials at elevated temperatures.

Taking into account that both Li–Ni exchange and Li_2MnO_3 formation are strongly influenced by various synthesis and processing parameters, the considerable dependence of electrochemical performance of Li–Ni–Mn–O-based cathode materials on their thermal and chemical prehistory should be observed. It is proved to be especially

* Corresponding author. Tel.: +82 2 2049 6042; fax: +82 2 452 5558.
E-mail address: ysyoon@konkuk.ac.kr (Y.S. Yoon).

0378-7753/$ – see front matter © 2004 Elsevier B.V. All rights reserved.
doi:10.1016/j.jpowsour.2004.08.052

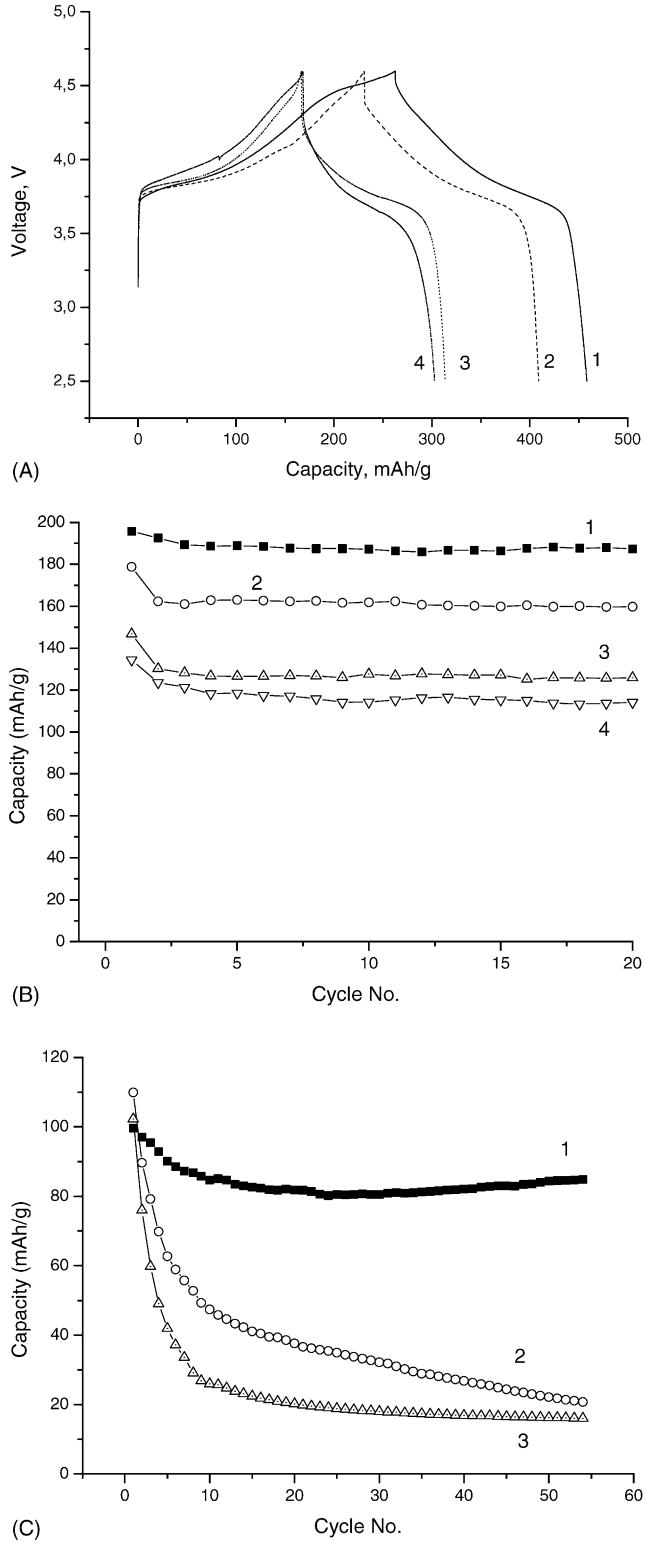

Fig. 1. Charge–discharge curves for the 1st cycle (A); specific discharge capacities at $I = 0.1\,\mathrm{mA\,cm^{-2}}$ (B) and $1\,\mathrm{mA\,cm^{-2}}$ (C) for LMN-based cathode materials. 1—$Li_{1.3}Ni_{0.5}Mn_{0.5}O_2$; 2–4—$LiNi_{0.5}Mn_{0.5}O_2$. Samples are obtained from hydroxide precursors (1, 2) or from acetate (3) and nitrate–acetate (4) solutions. Annealing duration at 900 °C is 1 h.

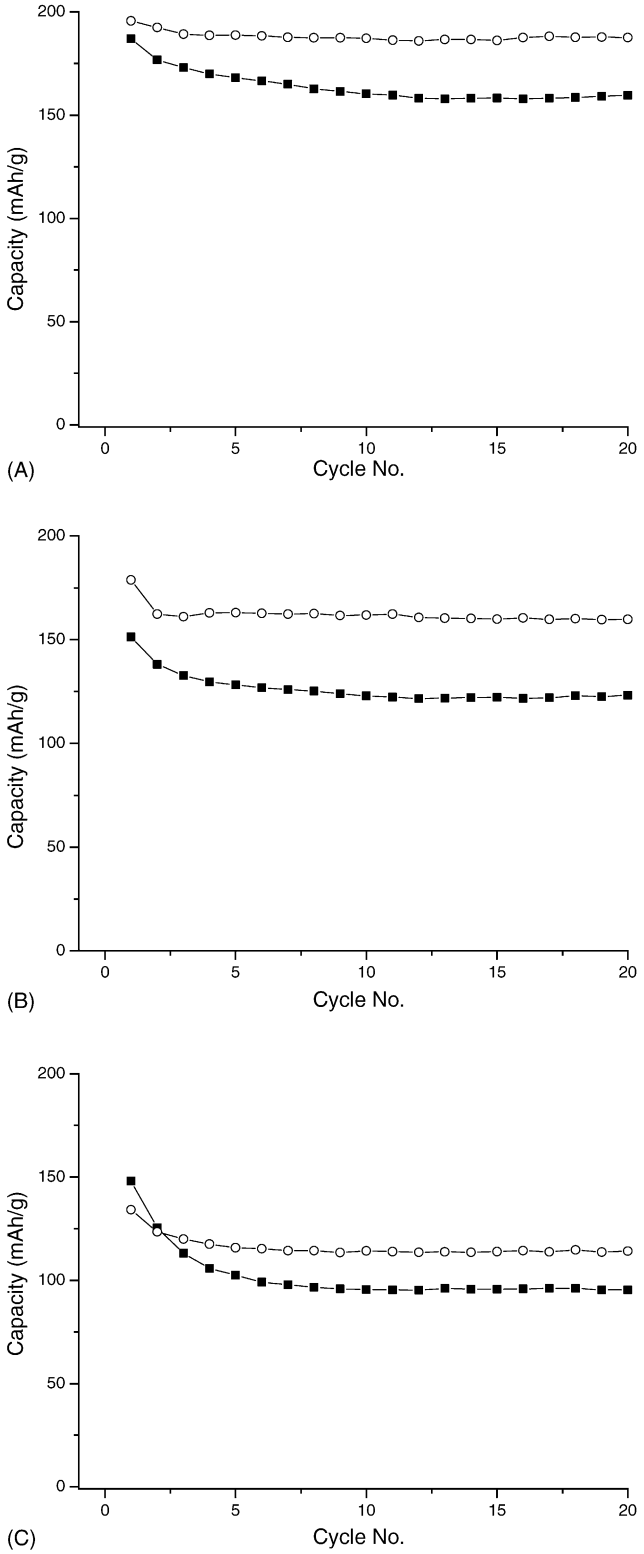

Fig. 2. The influence of HT-annealing duration on the discharge capacity of cathode materials. (A) $Li_{1.3}Ni_{0.5}Mn_{0.5}O_2$ (hydroxides); (B) $LiNi_{0.5}Mn_{0.5}O_2$ (hydroxides); (C) $LiNi_{0.5}Mn_{0.5}O_2$ (nitrate + acetates). Annealing time is: 1 h (empty symbols) and 12 h (filled symbols). $I = 0.1\,\mathrm{mA\,cm^{-2}}$.

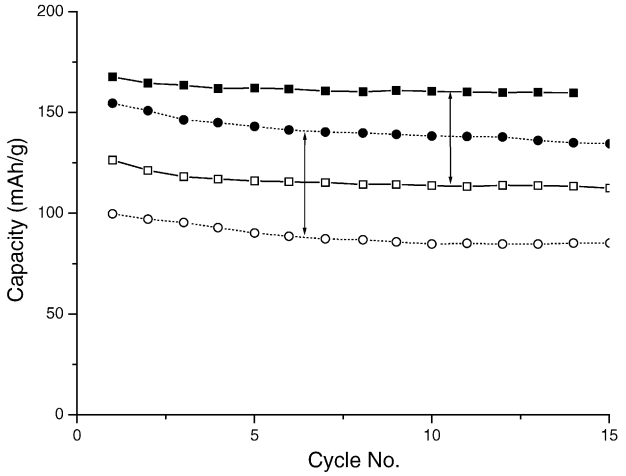

Fig. 3. Discharge capacity of $Li_{1.3}Ni_{0.5}Mn_{0.5}O_2$ (hydroxide prehistory) at higher discharge currents. $I = 0.5\,mA\,cm^{-2}$ (squares) and $1\,mA\,cm^{-2}$ (circles). HT-annealing duration: 1 h (filled symbols) and 12 h (empty symbols).

important for $LiNi_{0.5}Mn_{0.5}O_2$-based cathodes. According to various papers, the discharge capacity of the last ones is varied from 90 to 200 mAh g^{-1} at similar thermal processing conditions and discharge rates [1,2,6–9]. At the same time, the need in the new generation of cathode materials, based on Li–Ni–Mn oxides and exceeding the electrochemical performance of $LiCoO_2$, demands establishing reliable correlations between functional parameters of cathode materials and their synthesis conditions. The studies in this field allowed us to make several interesting and practically important observations reported in the present paper.

2. Experimental

Powders of $LiNi_{0.5}Mn_{0.5}O_2$ have been prepared by freeze-drying method using various precursor compositions. During the synthesis by solution scheme Li acetate or nitrate and Ni and Mn acetates were dissolved in water in the stoichiometric ratio. The solution was frozen by spraying to liquid nitrogen via pneumatic nozzle and freeze-dried at $P = 5 \times 10^{-2}$ mbar (Alpha 2–4, Christ) for 1–2 days.

According to precipitation scheme, which can be considered as modified "hydroxide method" [19], Ni and Mn acetate were mixed in the stoichiometric ratio and dissolved in water. 1 M solution of NaOH was added under stirring until pH 10; coprecipitated (Ni, Mn) hydroxide was filtered and carefully washed by deionized water. Frozen Ni–Mn hydroxides were placed to freeze-drier at $P = 5 \times 10^{-2}$ mbar (Alpha 2–4, Christ) for 1 day. The amount of ($OH^- + H_2O$) in the residue was determined by gravimetric method. Necessary amount of $LiOH{\cdot}H_2O$, calculated using gravimetric analysis data, was mixed with freeze-dried Ni–Mn hydroxide in the ball mill. Along with $LiNi_{0.5}Mn_{0.5}O_2$, the composition with superstoichiometric amount of lithium ($Li_{1.3}Ni_{0.5}Mn_{0.5}O_{2+y}$) was also prepared by this method.

Thermal decomposition of precursor powders, obtained using both schemes, was realized by fast heating of precursor powders (solution scheme) or pellets to 500 °C followed by 8-h dwelling. As-obtained powders (or crushed pellets) were pressed to pellets and placed for various time to muffle furnace preheated to 900 °C. Cooling of samples was performed by air quenching. $Li_{1+x}Ni_{0.5}Mn_{0.5}O_{2+\delta}$ (LMN) powders,

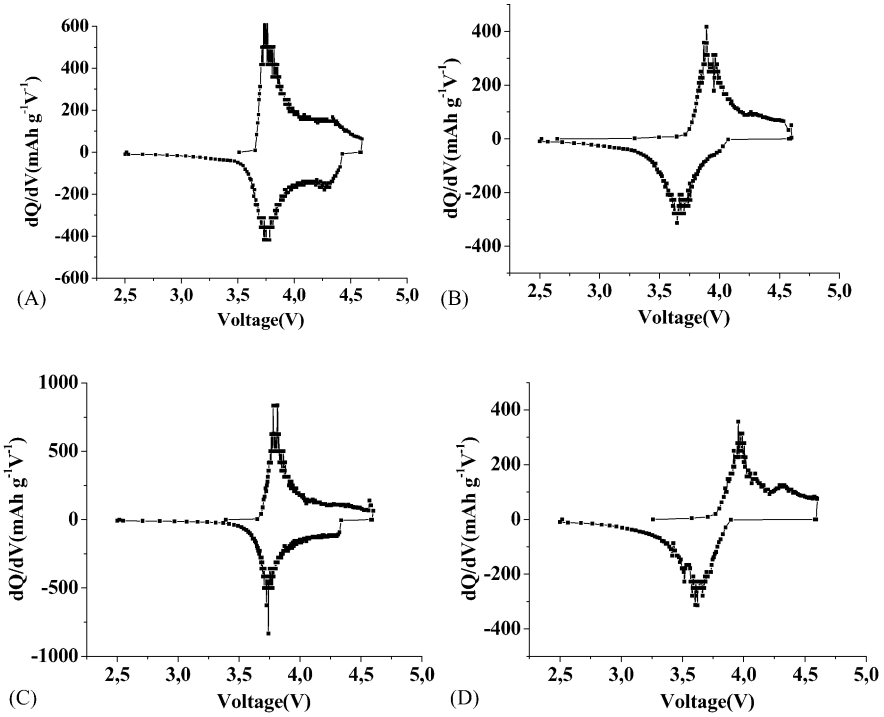

Fig. 4. Differential capacity vs. voltage curves. (A, C) $Li_{1.3}Ni_{0.5}Mn_{0.5}O_2$ (hydroxide prehistory) and (B, D) $LiNi_{0.5}Mn_{0.5}O_2$ (acetate prehistory). HT annealing duration: 1 h (A, B) and 12 h (C, D).

obtained by grinding the quenched pellets, have been studied by XRD (Geigerflex, Rigaku, 2° min^{-1}, Cu Kα), SEM (Philips ESEM) and TEM (Philips CM-30, $U = 200$ kV).

The electrochemical characterizations were performed using CR2032 coin-type cell; cut-off voltage 2.5–4.6 V, $I = 0.1$ mA. The cathode was fabricated with 20 mg of accurately weighed active material ($Li_{1+x}Ni_{0.5}Mn_{0.5}O_2$) and 12 mg of conductive binder (8 mg of Teflonized acetylene black (TAB) and 4 mg graphite). It was pressed on 200 mm^2 stainless steel mesh used as the current collector under a pressure of 300 kg cm^{-2} and dried at 180 °C for 24 h in a vacuum oven. The test cell was made of cathode and lithium metal anode separated by a porous polypropylene film (Celgard 3401). The electrolyte used was 1 M $LiPF_6$ in ethylene carbonate (EC)/dimethyl carbonate (DMC) mixture (1:2 by vol., Merck).

3. Results and discussion

Analysis of charge–discharge curves of electrochemical cells, prepared using obtained LMN powders, confirmed that the maximum electrochemical capacity values are observed for the $Li_{1+x}Ni_{0.5}Mn_{0.5}O_{2+\delta}$ samples with $x > 0$, as it was found in [15] (Fig. 1A and B). The introduction of superstoichiometric lithium into $LiNi_{0.5}Mn_{0.5}O_2$ leads also to the stabilization of discharge capacity values during further cycling at the considerably higher level than for samples with stoichiometric amount of Li. The difference is especially significant at higher discharge rates (Fig. 1C).

LMN materials containing stoichiometric amount of lithium ($LiNi_{0.5}Mn_{0.5}O_2$) demonstrate rather diverse electrochemical behavior. The highest and the most reproducible discharge capacity values are displayed by the sample, obtained by modified hydroxide method, while the capacity of samples obtained using solution scheme is considerably lower (Fig. 1B). Taking into account the mechanism of Li(Ni, Mn)O_2 phase formation, described in [18], these difference can be attributed to the different ratio of Li_2MnO_3 and $LiNi_{0.5}Mn_{0.5}O_2$ in the intermediate thermolysis products of hydroxide (precipitation scheme) and acetate (solution scheme) precursors. Larger amount of Li_2MnO_3 during the decomposition of acetate precursors, caused by features of its thermal decomposition mechanism, should complicate further crystallographic ordering of $LiNi_{0.5}Mn_{0.5}O_2$ phase during final annealing at 900 °C due to poorer chemical homogeneity of system after thermal decomposition.

Along with peculiarities, caused by different Li content or by different chemical prehistory of LMN powders in study, several important features, which can be inherent to all Li–Ni–Mn oxide-based cathode materials, were observed. The highest electrochemical capacity of other polycrystalline cathode materials with hexagonal structure similar to α-$NaFeO_2$ is commonly realized at the maximum level of crystallographic ordering, usually achieved by continuous isothermal annealing at elevated temperatures. According to these observations, continuous annealing at $T \geq 900$ °C was used in several works for producing Li(Ni, Mn)O_2-based cathode materials. At the same time, the experimental evaluation of the influence of annealing duration on the electrochemical performance of LMN materials clearly shows that all samples irrespective of Li stoichiometry and chemical prehistory demonstrated significantly higher capacity values for lower duration of high-temperature processing (Fig. 2). The effect is well reproducible; the increase of discharge rate, along with common decrease of capacity values, promotes further enhancement of this difference (Fig. 3).

The evaluation of differential capacity curves (Fig. 4) does not make clear the reasons of unusual high-temperature processing effect, as none of the observed differences can be unambiguously associated with changes in LMN-based cathode materials during annealing at 900 °C. Positions of the main oxidation and reduction maxima display correlation only with

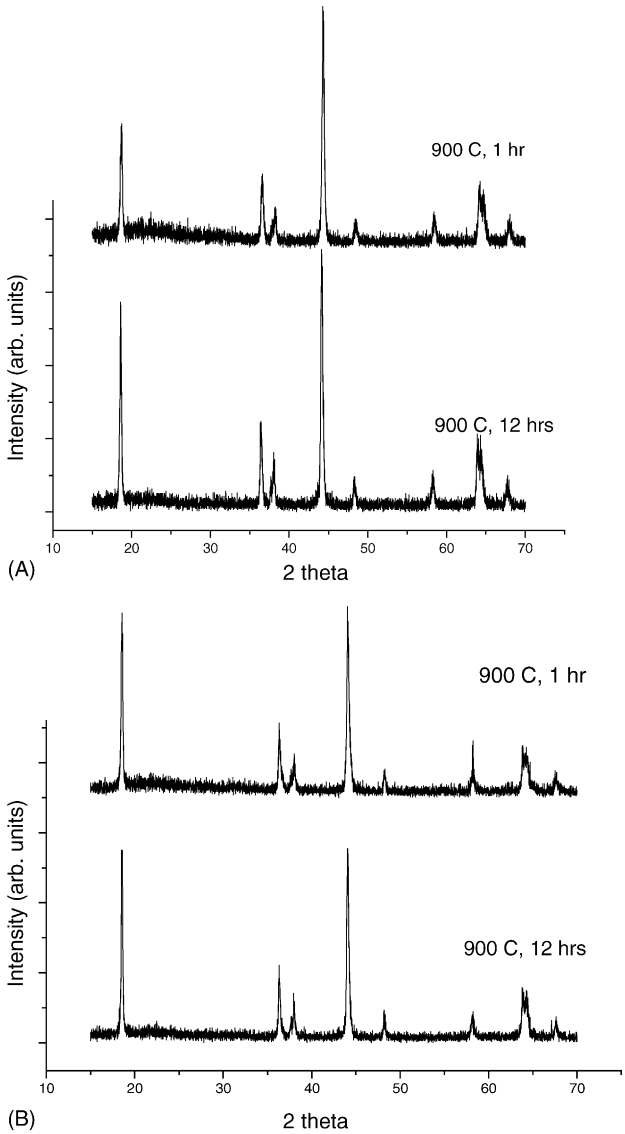

Fig. 5. XRD patterns of (A) $Li_{1.3}Ni_{0.5}Mn_{0.5}O_2$ (hydroxide prehistory) and (B) $LiNi_{0.5}Mn_{0.5}O_2$ (acetate prehistory).

chemical prehistory of samples. The distance between these peaks is ~0.3 V for powders with acetate prehistory and close to zero for hydroxide-based samples, irrespective of Li content and annealing duration. This smaller difference between oxidation and reduction peaks positions shows at the better reversibility of Li intercalation processes in these samples which, in turn, ensures reduced capacity fade during battery cycling.

XRD patterns of obtained $Li_{1+x}Ni_{0.5}Mn_{0.5}O_2$ powders (Fig. 5) also demonstrate the absence of considerable difference between powders with different Li content, chemical prehistory or HT annealing duration. All samples are single phase with hexagonal structure of α-$NaFeO_2$-type (space group $R\bar{3}m$) similar to high-temperature polymorph of $LiCoO_2$. Apart from $Li[Ni_xLi_{(1/3-2x/3)}Mn_{(2/3-x/3)}]O_2$ powders, little or no traces of reflections at 22–25°, attributed to Li_2MnO_3 [12,13] or to short-ranged superlattice ordering [8,9], was found either in $LiNi_{0.5}Mn_{0.5}O_2$ or in $Li_{1.3}Ni_{0.5}Mn_{0.5}O_2$ samples. At the same time splitting of 0 1 8/1 1 0 reflections at 64–65° shows at significant crystallographic ordering in LMN samples even after 1 h annealing at 900 °C.

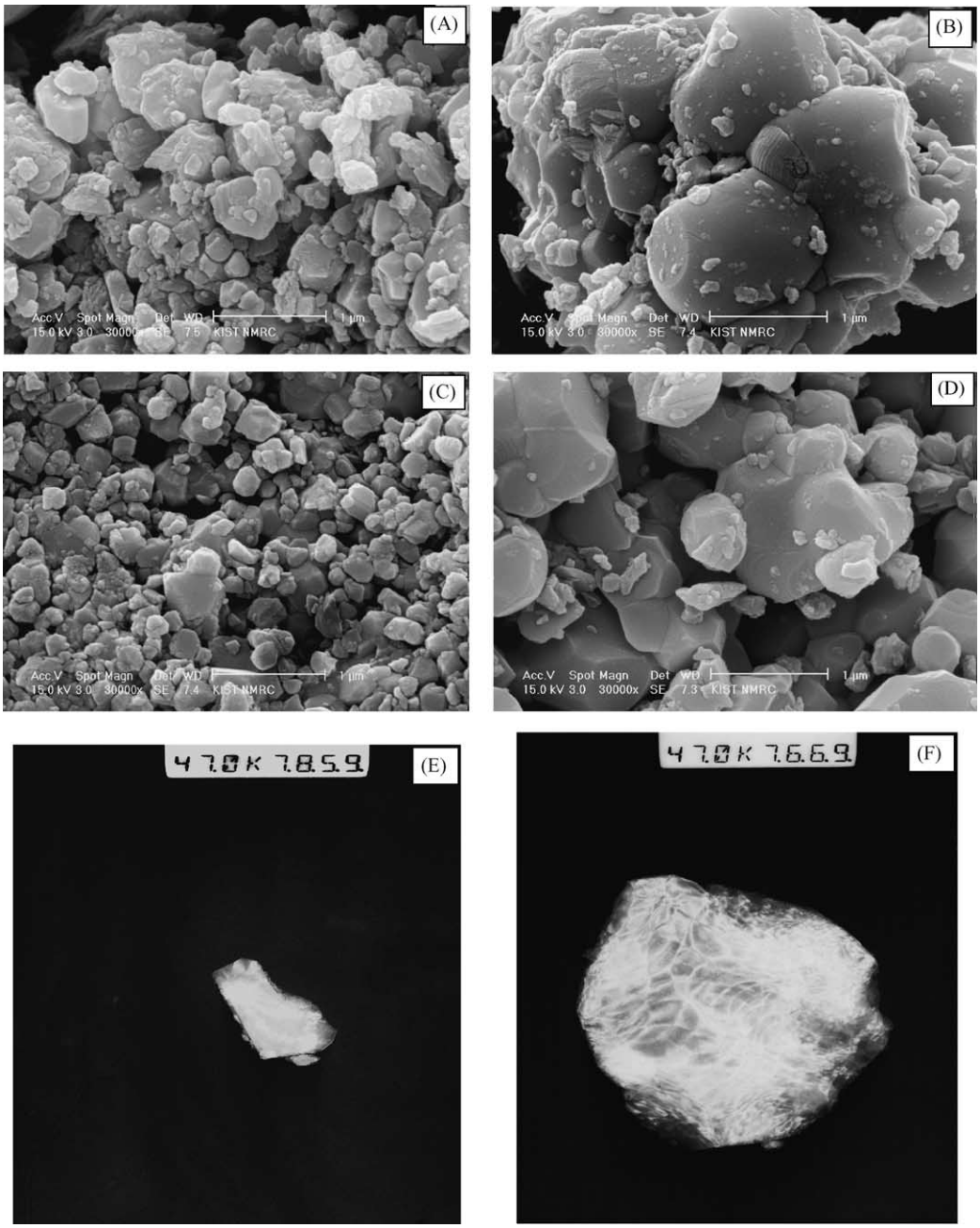

Fig. 6. SEM (A–D) and TEM (E, F) micrographs of LMN powders after thermal processing at 900 °C for: 1 h (A, C, E) and 12 h (B, D, F). (A, B) $Li_{1.3}Ni_{0.5}Mn_{0.5}O_2$ (hydroxide prehistory) and (C–F) $LiNi_{0.5}Mn_{0.5}O_2$ (acetate prehistory).

The most obvious effect of high-temperature processing duration on LMN powder properties was observed during morphological studies. Taking into account that thermal decomposition of freeze-dried precursors usually results in the formation of submicron oxide powders [20] and having regard to considerable rate of diffusion processes in Li–Ni–Mn oxides at 900 °C, it can be concluded that continuous processing at this temperature should be accompanied by considerable grain growth. Indeed, SEM analysis of LMN powders demonstrated the drastic difference in size of powder crystallites of LMN samples with both acetate and hydroxide prehistories (Fig. 6A–D). Meanwhile, there is no evidence that grain growth process at 900 °C is accompanied by substantial crystallographic ordering. Bright-field TEM images of powder grains (Fig. 6E and F) indicate the presence of considerable number of defects in both 1 and 12 h annealed samples.

The phenomenon similar to the observed capacity decrease of LMN cathode materials caused by high-temperature processing was observed in [12]. Rising final processing temperature from 900 to 1000 °C was accompanied by systematic reduction of reversible discharge capacity values. This decrease was associated with faster annealing of defects during thermal processing at elevated temperatures and partial conversion of distorted $Li[Li_{0.1}Ni_{0.35}Mn_{0.55}]O_2$ into structurally stable but less active electrochemically secondary phases ($Li_2Mn_2O_4$, Li_2MnO_3). Instead, significant enhancement of cationic disorder, caused by rising processing temperature since 900–1000 °C, was found in $LiNi_{0.4}Mn_{0.4}Co_{0.2}O_2$ using Rietveld refinement technique [21]. This structural disordering was also accompanied by significant capacity decrease.

Thermal processing in the present study was performed at 900 °C, so that the factors promoting capacity decrease during annealing at 1000 °C should be insignificant. It should be noted, however, that considerable number of defects after 12 h annealing at 900 °C (Fig. 6F) shows that the defect-related capacity fall cannot be completely excluded. Meanwhile, another explanation of capacity decrease during isothermal annealing seems more probable. The most obvious powder parameter which, along with discharge capacity, clearly changes in the course of annealing is the size of LMN crystallites. Substantial influence of discharge rate on the reversible capacity values of obtained powders indicates that one of the factors limiting the effective capacity level is rather low rate of Li diffusion in the LMN crystallites. In this case, smaller size of crystallites ensures shorter mean length of Li diffusion pathways from its position in the LMN lattice to the cathode–electrolyte interface. Shorter diffusion distances promote faster and more uniform Li intercalation into LMN crystallites during discharge process compared to coarse-grained samples, thus increasing effective capacity values. According to this mechanism, the influence of particle size effect should increase with growing discharge rates that correlate quite well with experimental observations (Fig. 3).

4. Concluding remarks

Performed experiments demonstrated that the electrochemical performance of $Li_{1+x}Ni_{0.5}Mn_{0.5}O_{2+\delta}$ cathode materials is controlled by several independent factors. The first and the most important of them is Li stoichiometry; samples with $x > 0$ demonstrated considerably higher capacity values. Another important factor is chemical prehistory of materials. Complicated crystallographic ordering processes in the multicomponent oxide materials at moderate temperatures make the influence of chemical homogeneity of precursor decomposition products and, thus, chemical prehistory of materials especially significant at higher discharge rates. Unusual behavior of $Li_{1+x}Ni_{0.5}Mn_{0.5}O_{2+\delta}$ during annealing at 900 °C, when continuous processing promotes not enhancement but decrease in capacity values, seems to be the general feature of Li–Ni–Mn–O-based cathode materials and can be explained by drastic influence of particle size effect in materials with moderate rates of solid-state transport of lithium. Generally, apart from many other works where the features of electrochemical behavior of LMN-based cathode materials were explained only from crystallochemical point of view, the present work demonstrated that their electrochemical performance is substantially controlled by kinetic and processing-related factors. Further optimization and enhancement of the properties of $Li_{1+x}(Ni, Mn)O_{2+\delta}$ cathode materials need more detailed studies of the influence of synthesis and processing conditions on their functional parameters.

Acknowledgment

We would like to appreciate the support by National Research Laboratory Program (development of monolithic high-power hybrid battery) and Brain Pool/KISTEP fellowship (O.A. Shlyakhtin) of the Ministry of Science and Technology, Republic of Korea.

References

[1] T. Ohzuku, Y. Makimura, Chem. Lett. (2001) 744.
[2] B.L. Cushing, J.B. Goodenough, Solid State Sci. 4 (2002) 1487.
[3] R. Chitrakar, S. Kasaishi, A. Umeno, K. Sakane, N. Takagi, Y.-S. Kim, K. Ooi, J. Solid State Chem. 169 (2002) 35.
[4] X.-Q. Yang, J. McBreen, W.-S. Yoon, C.P. Grey, Electrochem. Commun. 4 (2002) 649.
[5] L. Zhang, H. Noguchi, M. Yoshio, J. Power Sources 110 (2002) 57.
[6] Y.-K. Sun, C.S. Yoon, Y.S. Lee, Electrochim. Acta 48 (2003) 2589.
[7] K.M. Shaju, G.V. Subba Rao, B.V.R. Chowdari, Electrochim. Acta 48 (2003) 1505.
[8] Z. Lu, D.D. MacNeil, J.R. Dahn, Electrochem. Solid State Lett. 4 (2001) 191.
[9] Z. Lu, L.Y. Beaulieu, R.A. Donaberger, C.L. Thomas, J.R. Dahn, J. Electrochem. Soc. 149 (2002) 778.
[10] Z. Lu, J.R. Dahn, J. Electrochem. Soc. 149 (2002) 815.
[11] S.-S. Shin, Y.-K. Sun, K. Amine, J. Power Sources 112 (2002) 634.

[12] J.-H. Kim, C.S. Yoon, Y.-K. Sun, J. Electrochem. Soc. 150 (2003) 538.
[13] J.-H. Kim, Y.-K. Sun, J. Power Sources 119–121 (2003) 166.
[14] Y.J. Park, M.G. Kim, Y.-S. Hong, X. Wu, K.S. Ryu, S.H. Chang, Solid State Commun. 127 (2003) 509.
[15] O.A. Shlyakhtin, Y.S. Yoon, S.-H. Choi, Y.-J. Oh, Electrochim. Acta (2004).
[16] R. Stoyanova, E. Zhecheva, R. Alcantara, J.L. Tirado, G. Bromiley, F. Bromiley, T. Boffa Balaran, Solid State Ionics 161 (2003) 197.
[17] W.-S. Yoon, N. Kim, X.-Q. Yang, J. McBreen, C.P. Grey, J. Power Sources 119–121 (2003) 649.
[18] M. Yoshio, Y. Todorov, K. Yamato, H. Noguchi, J. Itoh, M. Okada, T. Mori, J. Power Sources 74 (1998) 46.
[19] Z. Lu, J.R. Dahn, J. Electrochem. Soc. 148 (2001) 237.
[20] Yu.D. Tretyakov, N.N. Oleinikov, O.A. Shlyakhtin, Cryochemical Technology of Advanced Materials, Chapman & Hall, London, 1997.
[21] J. Katana Ngala, N.A. Chernova, M. Ma, M. Mamak, P.V. Zavalij, M. Stanley Whittingham, J. Mater. Chem. 14 (2004) 214.